

First-principles study of the stability and electronic structure of metal hydridesH. Smithson,^{1,2} C. A. Marianetti,¹ D. Morgan,¹ A. Van der Ven,¹ A. Predith,¹ and G. Ceder¹¹*Department of Materials Science and Engineering, Massachusetts Institute of Technology, Cambridge, Massachusetts 02139*²*Department of Materials Science and Metallurgy, University of Cambridge, Pembroke Street, Cambridge CB2 3QZ, United Kingdom*

(Received 10 March 2002; revised manuscript received 30 July 2002; published 21 October 2002)

A detailed analysis of the formation energies for alkali, earth-alkali, and transition-metal hydrides is presented. The hydriding energies are computed for various crystal structures using density functional theory. The early transition metals are found to have a strong tendency for hydride formation which decreases as one goes to the right in the transition-metal series. A detailed analysis of the changes in band structure and electron density upon hydride formation has allowed us to understand the hydriding energy on the basis of three contributions. The first is the energy to convert the crystal structure of the metal to the structure formed by the metal ions in the hydride (fcc in most cases). In particular, for metals with a strong bcc preference such as V and Cr, this significantly lowers the driving force for hydride formation. A second contribution, which for some materials is dominant, is the loss of cohesive energy when the metal structure is expanded to form the hydride. This expansion lowers the cohesive energy of the metal and is a significant impediment to form stable hydrides for the middle to late transition metals, as they have high cohesive energies. The final contribution to the hydride formation energy is the chemical bonding between the hydrogen and metal in which it is inserted. This is the only contribution that is negative and hence favorable to hydride formation.

DOI: 10.1103/PhysRevB.66.144107

PACS number(s): 61.50.Ah, 61.66.Dk

I. INTRODUCTION

The absorption of hydrogen in materials is of wide and universal importance. In many metals, it can lead to premature failure under stress,¹ a phenomena referred to as hydrogen embrittlement. The mechanism of such embrittlement is believed to be different depending on whether or not stable hydrides can be formed. Metal hydrides are also important as a potential hydrogen source for small portable fuel cells.² Reversible hydriding can be used as a fuel storage mechanism for operation with large fuel cells for stand-alone power or for automobiles.³

Hydrides for hydrogen storage need to be able to form hydrides with a high hydrogen-to-metal ratio, but should not be too stable, so that the hydrogen can easily be released without excessive heating. Magnesium and magnesium-nickel hydrides contain a relatively high fraction of hydrogen by weight, but need to be heated to at least 250 or 300 °C in order to release the hydrogen. Nickel-metal hydrides for rechargeable batteries are even more demanding and require reversible hydrogen exchange at room temperature. Metastable hydrides, such as AlH₃, can be useful as a one-time hydrogen source for small portable power application. Understanding the stability of metal hydrides is therefore key to rationally investigate and design potential hydrogen-storage materials. The central objective of this paper is to explain the stability of hydrides on the basis of the electronic structure. Using modern first-principles energy computations, the energy for hydride formation is calculated for a large number of metals. By systematically breaking the hydride formation energy down into several pieces, the trend across the transition metals is explained. It is demonstrated that the electronic structure of the host metal is a key factor in determining the stability of the hydride.

II. LITERATURE SURVEY

Table I shows a compilation of hydride stability across the periodic table. All the common alkali metals form a monohydride with the rocksalt structure. MgH₂ forms a rutile structure though a fluorite MgH₂ has been claimed at high pressure.⁴ The other earth alkalis form dihydrides in the Co₂Si-type structure. Among the transition metals, mainly the early transition metals form stable hydrides. For these the fluorite structure is the dominant crystal structure. The rare earths form the fluorite structure. Hydrogen can be added to the dihydrides of La and Y to form a trihydride with the BiF₃ structure. The BiF₃ structure can be derived from the fluorite structure by inserting H into the octahedral positions of the fcc metal sublattice. The ThH₂ structure formed at low temperature for Ti, Zr, and Hf is a tetragonally distorted variant of the fluorite structure. The bcc metals V, Nb, and Ta all form solid solutions of H within the bcc metal above a certain temperature. At higher H concentration, Nb and V form the dihydride with fluorite structure. The mid-to-late transition metals do not form stable hydrides under normal conditions, indicating that their formation energy is positive. However, some are known to form hydrides at high H₂ pressure, which suggests that for those cases the formation energies are probably quite small. CuH is metastable and has been claimed to have the wurtzite structure.⁵ Zn and Cd hydrides can be synthesized, but are metastable and their structure is unknown.⁶ Only a few main-group elements form stable solid hydrides. Al forms a metastable hydride and InH₃ polymerizes.⁷ Hence these main-group elements will not be discussed further in this study.

There is general agreement that the hydrides of the alkali and earth-alkali metals are ionic with a strongly negatively charged anionic hydrogen.⁷ The hydrogen-metal interaction in transition-metal hydrides is less clear, and even the charge

TABLE I. Compilation of known hydrides for the transition metals and groups IA, IIA, and IIB. Most data from Refs. 2, 3, and 24. High-pressure MgH₂ from Ref. 4. MoH and FeH information from Ref. 5.

Li LiH (rocksalt)	Be BeH ₂										
Na NaH (rocksalt)	Mg MgH ₂ (rutile) MgH ₂ (fluorite) at high P										
K KH (rocksalt)	Ca CaH ₂ (Co ₂ Si)	Sc ScH ₂ (fluorite)	Ti TiH ₂ (fluorite) TiH ₂ (TiH ₂) at low T	V V ₂ H, V ₃ H ₂ , VH (H interstitial solution in bcc V) VH ₂ (fluorite)	Cr CrH (NIAs) at high P CrH ₂ (fluorite) CrH ₃	Mn MnH (NIAs)	Fe FeH (double hexagonal) at high P, low T	Co CoH, CoH ₂ P > 50 MPa	Ni NiH ₂ (non-stoichiometric rocksalt)	Cu CuH (wurtzite)	Zn unstable hydrides
Rb RbH (rocksalt)	Sr SrH ₂ (Co ₂ Si)	Y YH ₂ (fluorite) YH ₃ (BiF ₃)	Zr ZrH ₂ (fluorite) ZrH ₂ (ThH ₂) at low T	Nb Nb ₂ H (H interstitial in Nb) NbH (struc. unknown) NbH ₂ (fluorite)	Mo MoH (NIAs) at high P	Tc	Ru	Rh RhH (CsCl) at high P	Pd Pd ₂ H ₂ PdH ₂ (NiMo ₄)	Ag	Cd unstable hydrides
Cs CsH (rocksalt)	Ba BaH ₂ (Co ₂ Si) T < 600°C	La LaH ₂ (fluorite) LaH ₃ (BiF ₃)	Hf HfH ₂ (ThH ₂) HfD ₂ has fluorite structure	Ta Multiple interstitial ordering phases, most below 0°C	W	Re	Os	Ir	Pt	Au	Hg unstable hydrides

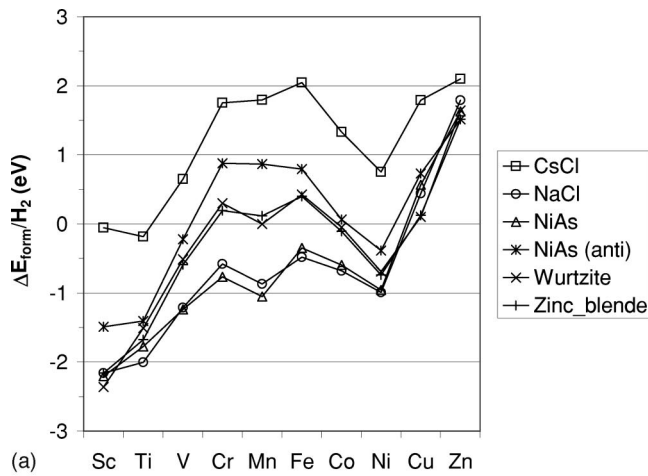
of the hydrogen in these materials has been under dispute. The high mobility of hydrogen in many metals and their magnetic behavior have been taken as evidence for a protonic (i.e., H⁺) model with the hydrogen electronic states far above the transition-metal states.⁸ This viewpoint was corrected when the first electronic structure computations on hydrides appeared.^{9–11} While these computations were non-self-consistent, they clearly showed that hydrogen not only contributes electrons to the system, but also states below the bottom of the metal *d*-band. Wallace and Malik¹² used the electronic structure calculations of Switendick to explain the stability of the monohydrides by the hybridization of the H 1s state with the *s* and *p* states of the metal, with no particular role for the metal *d* states. In the dihydrides, on the other hand, it was argued that the two hydrogen atoms per unit cell would form both their bonding and antibonding band below the bottom of the *d* band.¹² Hence, by contributing states below the Fermi level, the electrons of the host can lower their energy by transferring to these new levels. As the hydride contracts, the antibonding band moves up. It was suggested that when this band moves above the top of the *d* band the dihydride is not stable anymore. This has been used to explain why hydrides with small lattice parameter, such as PdH₂ are not stable as dihydrides.

Since these early calculations, hydrides have continued to be fertile ground for first-principles electronic structure computations. Papaconstantopoulos and Switendick¹³ indicated the importance of self-consistency in charge density and potential for first-principles computations. More recently MgH₂ has been investigated with the Hartree-Fock¹⁴ and the local density approximation (LDA) pseudopotential approach.¹⁵ One of the most detailed recent investigations into the electronic structure of cubic and tetragonal hydrides was performed by Wolf and Herzog.¹⁶ Gupta has investigated hydrides of intermetallic compounds.¹⁷ Most of these studies have focused on the electronic structure of the hydrides without relating it to their energy of formation, which is the criti-

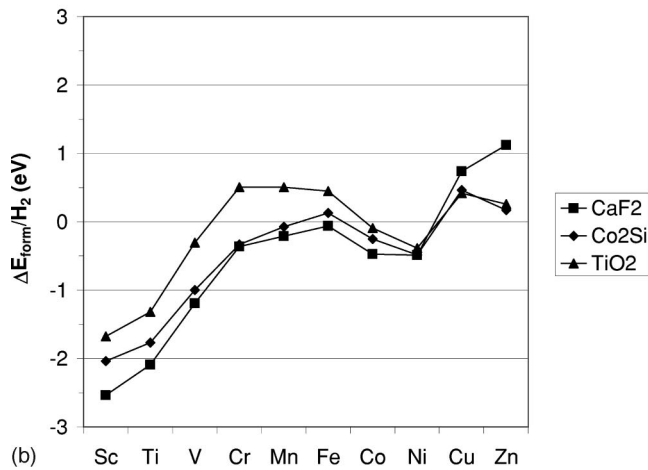
cal property for most applications. Miedema used empirical correlations to deduce the rule of “reverse stability.”¹⁸ He argued that the more stable the metal alloy, the less stable the hydride. This has been interpreted in terms of the breaking of metal-metal bonds by the insertion of hydrogen: the more stable the metal alloy, the harder it is to replace some of these bonds with metal-H bonds. Understanding the hydride formation energy through its relation with the electronic structure is the focus of this paper.

III. COMPUTATIONAL DETAILS

All computations were performed in the local density approximation (LDA) to density functional theory. Atomic cores are represented with ultrasoft pseudopotentials as implemented in the Vienna Ab Initio Simulation Package (VASP).^{19,20} An energy cutoff of 300 eV was used for all hydride calculations and *k*-point sampling was performed on a 12×12×12 grid for all structures with the exception of the Co₂Si structure, for which a 6×6×6 grid was used. All structures were fully relaxed (cell parameters as well as internal geometries) so as to obtain the minimum of the total energy. All the calculations performed here were non-spin-polarized, even for cases known to be magnetic. We performed ferromagnetic spin-polarized calculations (using the local spin density approximation) for the first-row transition metals (from Sc to Ni) and their hydrides in the NaCl and fluorite structures to estimate the importance of spin polarization on the hydride formation energies. With the exception of Fe, Co, and Ni, inclusion of spin polarization has no effect on the hydride formation energies. While the hydride formation energies of Fe, Co, and Ni are quantitatively affected by spin polarization (the largest change was for FeH₂ of about 250 meV per CaF₂ unit cell) the qualitative trends predicted by the spin-polarized calculations do not differ from those predicted with the non-spin-polarized calculations. The alkali



(a)



(b)

FIG. 1. Formation energy for the monohydrides (a) and dihydrides (b) of the 3d transition metals in various crystal structures (reaction energy per H_2 molecule).

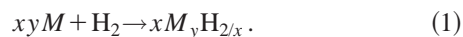
and alkali-earth metals are nonmagnetic and therefore do not require spin-polarized calculations.

IV. ELECTRONIC STRUCTURE AND FORMATION ENERGY OF TRANSITION-METAL HYDRIDES

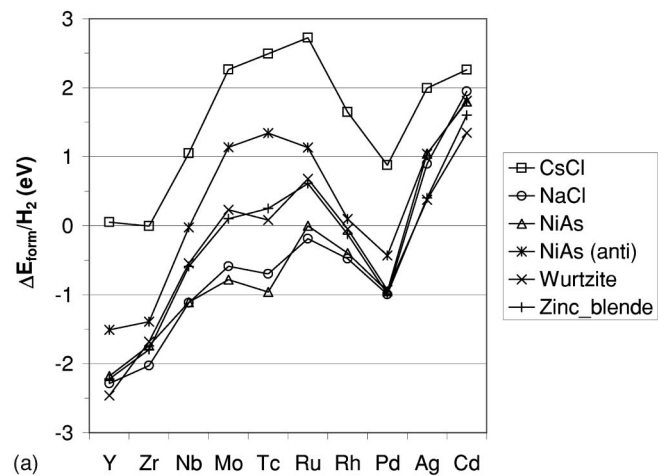
The transition-metal hydrides (and Zn and Cd hydrides) are studied as a group in this section since they have common features in their bonding and electronic structures. The alkali and alkali-earth hydrides will be discussed separately in Sec. VI.

A. Hydride formation energies and lattice parameters

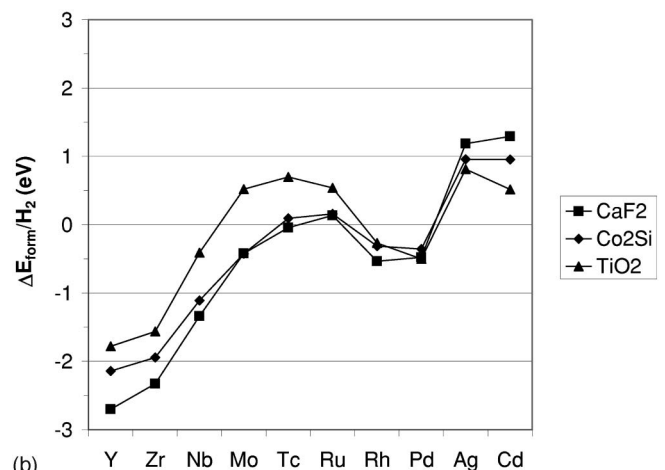
The stability of a hydride depends on its formation energy through the reaction



To compare the relative stabilities of hydrides, it is most useful to normalize all coefficients in the formation reactions per one molecule of H_2 . On this basis, the reaction energy is a measure of the H_2 chemical potential in equilibrium with



(a)



(b)

FIG. 2. Formation energy for the monohydrides (a) and dihydrides (b) of the 4d transition metals in various crystal structures (reaction energy per H_2 molecule).

the metal and hydride. The energy of the metal and metal hydride can be calculated with the density functional theory methods outlined in Sec. III. Determining the energy of H_2 gas is more difficult as it contains important entropy terms, and the LDA is known to make significant errors in the binding energy of small molecules. We therefore approximated the energy of H_2 by calculating the energy of an H_2 molecule in vacuum at zero K. The fact that this is only a rough approximation to the energy of real H_2 gas is not an impediment to our work, as we are mainly interested in relative energy differences between hydrides. Any shift in the energy of H_2 cancels out from such comparisons. However, because of the potential error on the H_2 energy, the “zero” of formation energy in Figs. 1 and 2 should only be taken as approximate. Another approximation in this work is that we neglect zero-point energies within the metal hydrides, a contribution to the total energy that can be large in hydrogen containing compounds due to the low mass of the hydrogen atom. In fact, first-principles calculations²¹ have indicated that the zero-point energy contribution can be as large as 250 meV per hydrogen atom in the fluorite structure. Nevertheless, the same first-principles study²¹ suggested that the value of the

TABLE II. Calculated lattice parameters for the $3d$ transition-metal hydrides in the rocksalt (NaCl) and fluorite (CaF_2) structures. Experimental values are indicated in brackets where available. Experimental data on ScH_2 , TiH_2 , and VH_2 from Ref. 23. NiH and CrH_2 lattice parameters are from Ref. 22.

Metal	Rocksalt	Fluorite
Sc	4.43	4.69 (4.78)
Ti	4.10	4.34 (4.44)
V	3.87	4.13 (4.27)
Cr	3.71	4.01 (3.86)
Mn	3.62	3.95
Fe	3.59	3.92
Co	3.60	3.92
Ni	3.64 (3.72)	3.98
Cu	3.79	4.20
Zn	4.15	4.48

zero-point energy depends more on the crystallographic site occupied by hydrogen (e.g., whether it is tetrahedral or octahedral) than on the transition metal. Hence the neglect of zero-point energies is not expected to modify predicted qualitative trends across the periodic table.

The monohydrides [Fig. 1(a)] and dihydrides [Fig. 1(b)] of the $3d$ and $4d$ [Figs. 2(a) and 2(b)] transition metals are calculated in several different structures, whether these structures have been observed experimentally or not, allowing for a systematic study of the independent effect of structure and metal chemistry. Most of the structures used in Figs. 1 and 2 have been observed experimentally as stable structures for some hydrides. The trends in Figs. 1 and 2 are quite similar and common to most of the structures. For the early transition metals the stability of the hydride rapidly decreases as one moves to the right in the transition-metal series. From the middle of the transition-metal series this trends levels off, with even a slight increase in stability upon further increase in d -electron count. Finally, the late transition metals, such as Cu and Ag, and the nontransition metals, such as Zn and Cd, have quite positive formation energy for their hydrides, implying that they are not likely to be stable.

Table II contains calculated lattice parameter data for the hydride rocksalt and fluorite structures. Whenever available, experimental data are given in parentheses. Given that computed lattice parameters are usually slightly underestimated by the local density approximation, the result for Cr is surprising and may hint at either an experimental or computational problem in this material.

B. Electronic structure of the hydrides

The electronic densities of states (DOS) for the $3d$ transition-metal hydrides are shown for the NaCl structure in Fig. 3 and for the CaF_2 structure in Fig. 4. The total DOS (solid line) is divided into a hydrogen s part (dotted line) and a metal d part (dashed line) by projection of the wave functions onto spheres surrounding the atoms. For both the metal and hydrogen, the sphere radius was chosen to be half the metal-hydrogen bond length. The characteristics for both

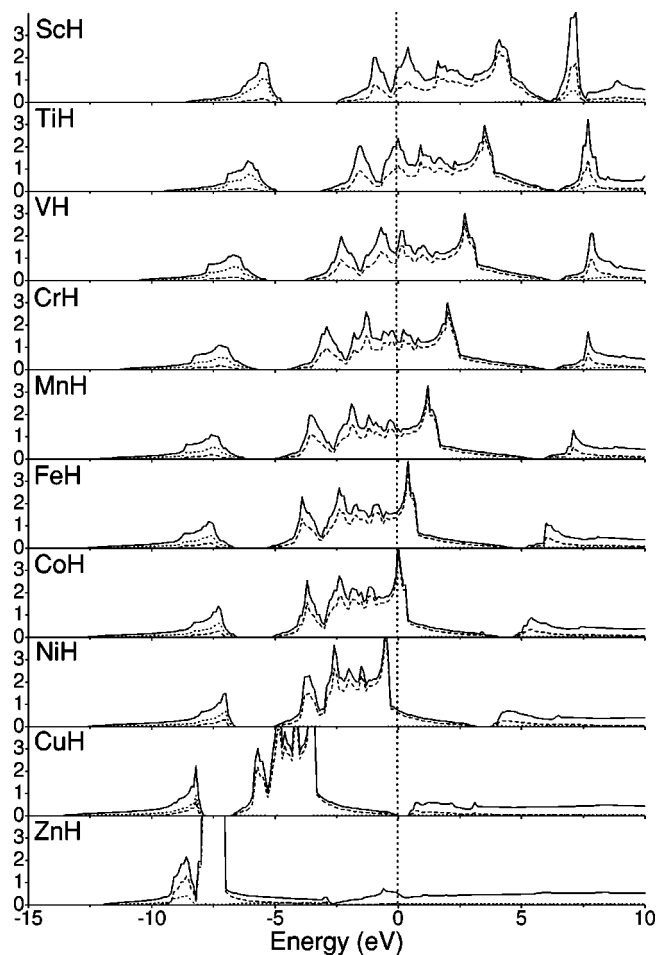


FIG. 3. Density of states for hydrides in the rocksalt structure. The solid line is the total DOS, the dotted line is the hydrogen $1s$ contribution, and the dashed line is the metal $3d$ contribution.

structures are quite similar. The hydrogen s part of the density of states is mainly concentrated in the low-energy region (approximately -8 eV below the Fermi level). In the monohydrides, the hydrogen character is isolated within the lowest peak, which is a single occupied band holding two electrons. As shown, this lowest band possesses significant hydrogen character, in addition to a characteristic free electron tail and some metal character. The metal character arises from the formation of bonding and antibonding orbitals between the metal e_g states and the hydrogen s . The hydrogen s character of the lowest band does begin to decrease later in the transition-metal series. For all the metals, except for Ni, Cu, and Zn, the Fermi level lies in the metal d states. As we move across the transition-metal series these metal d bands contract as the increased nuclear charge reduces the extent and overlap of the d orbitals, and the Fermi level moves up in the d band. In all figures, the Fermi level is referenced to zero.

More information can be gained by comparing the band structure of the metal and the hydride. Figure 5 shows the bands for titanium metal in the expanded fcc lattice (i.e., at the lattice parameter of TiH) and titanium hydride in the rocksalt structure. Similar band structures have been obtained for the other transition metals, but are not shown. The

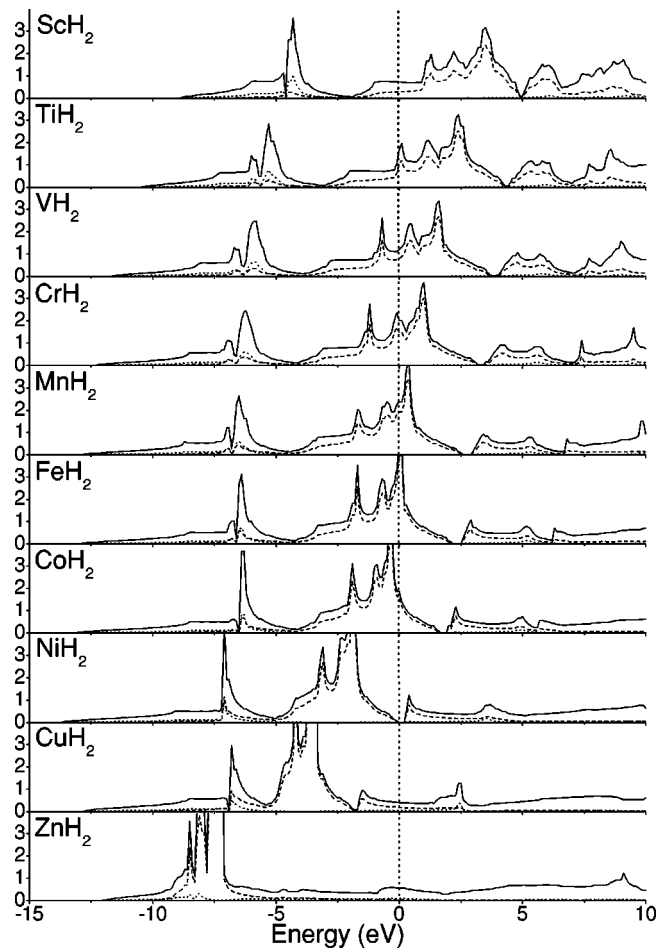


FIG. 4. Density of states for hydrides in the fluorite structure. The solid line is the total DOS, the dotted line is the hydrogen 1s contribution, and the dashed line is the metal 3d contribution.

bands near the Fermi level are the d bands of the metal (both in the pure metal and in the hydride). Although there is some difference between the e_g and t_{2g} bands at the Γ point, there is no significant crystal field splitting. As can be inferred from the figure, these bands are quite similar in the metal and in the metal hydride. The lowest band in the metal shows the characteristic free-electron-like behavior near the Γ point and crosses into the d bands. In the hydride, the free electron band from the metal hybridizes with the hydrogen s orbital, forming a bonding band which has shifted down in energy. Although these bands look similar, the character of the band has changed. In the hydride, this band possesses substantial hydrogen s character as can be seen in the projected density of states in Fig. 3, which is clearly not the case in the metal.

The changes in electron density upon hydriding can be visualized. First-principles computations result in single-particle wave functions for the system, which makes it possible to directly observe charge transfer and charge rearrangements upon hydrogen insertion into the metal. To separate the effect of H insertion from other changes to the structure, the difference in charge density between the hydride and the system of metal atoms in exactly the same position as in the hydride was calculated. For a hydride in the rocksalt or fluorite structure, the metal atoms form a fcc

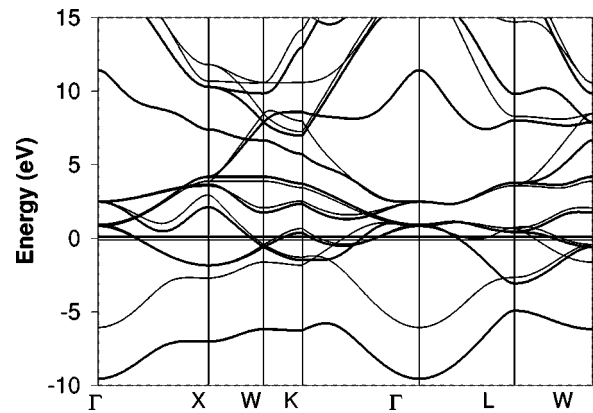


FIG. 5. Band structure of TiH (heavy line) in the rocksalt structure and fcc Ti (narrow line) with the same lattice parameter as the hydride.

structure, but at a lattice parameter larger than what would be observed if the metal alone were present. Hence we refer to this rocksalt structure without the hydrogen as the “expanded” metal structure. Using structures in which the metal atoms have exactly the same positions before and after hydrogen insertion allows us to subtract the charge density between the hydride and the metal point by point in space, thereby directly observing the charge density variations due to the hydrogen insertion. Figure 6 shows such charge density difference maps in the (001) plane of the rocksalt structure for several different metal hydrides. The light colored areas indicate electron gain, whereas the darker areas indicate electron loss. Because the electron gain on hydrogen is so much greater than on the transition metal, the minimum and maximum values of electron gain and loss were truncated at the values shown in the legend of Fig. 6 in order to keep enough resolution around the transition metals. Electron gain on the hydrogen position is substantial, indicating that the hydrogen does not insert as a bare proton. Near the transition metal there are both regions of positive and negative charge difference, corresponding to the loss or gain of d occupation. Significant loss of d occupation is only seen in the e_g orbitals, which is due to the formation of a bonding-antibonding pair between the directly overlapping hydrogen s and metal e_g orbitals. A more detailed understanding of which d orbitals gain occupation can be obtained by project-

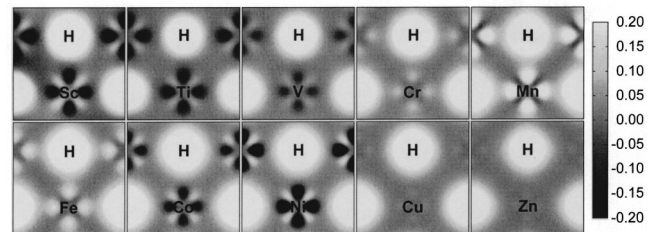


FIG. 6. Electron density change in the (001) plane as hydrogen is inserted into the metal with fcc structure. Difference is obtained by subtracting from the hydride density the electron density of metal with the same atomic positions. Light areas indicate where electron density is increased on adding hydrogen into the metal lattice.

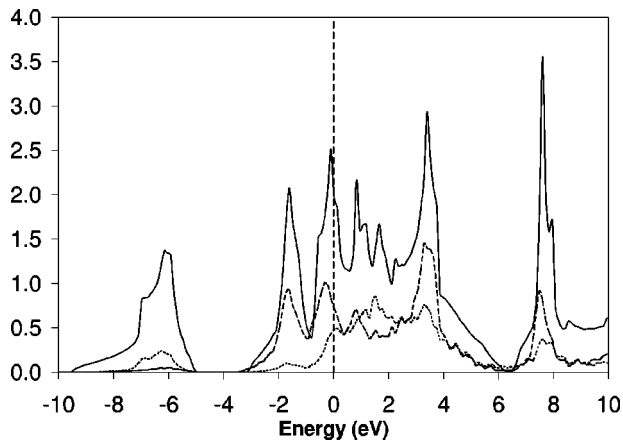


FIG. 7. Symmetry decomposed density of states for TiH in the rocksalt structure. The total (solid line) and projected t_{2g} (dashed line) and e_g (dotted line) density of states are shown.

ing the density of states onto the t_{2g} and e_g orbitals of the metal. This analysis will be critical to understanding the formation energy of the hydrides in Sec. V. For TiH the decomposed DOS is shown in Fig. 7, and the d states have been separated into t_{2g} and e_g symmetries. The t_{2g} states dominate the top and bottom of the d band with e_g states in the center of the band. This trend is consistent across the transition-metal series. The trend seen in the charge density plots can easily be explained if some amount of charge were being promoted to the Fermi surface. For the early transition metals, such as Sc, Ti, and V, hydriding puts extra charge in d states with t_{2g} character, as can be clearly seen in Fig. 6. The t_{2g} orbitals point away from the hydrogen. For Mn and Fe hydrides the Fermi level is near the center of the d band and the extra electron goes into e_g states. CrH is in between and has a weak gain in the e_g states. With Co and Ni the top of the d band is reached and filling occurs again in t_{2g} orbitals. Cu and Zn are somewhat different. In both the metal and hydride the d states are filled so that very little electron change occurs on the metal, and the electron gain is largely on hydrogen. One should keep in mind that in reality the Cu and Zn hydrides are very unstable, and if they form at all, it is likely to be in a structure different from the rocksalt. Metastable CuH has been synthesized⁵ and forms the wurtzite structure.

It is interesting to consider how H causes promotion (or demotion) of electrons to (from) the Fermi level of the metals. This will depend on whether H adds new states below the Fermi level, which is complicated to determine because of the hybridization between the metal and H. If the metal states involved in hybridization come from above the Fermi level or the antibonding states are added below the Fermi level, then two new states are added. On the other hand, if the metal states involved in hybridization come from below the Fermi level and the antibonding states are added above the Fermi level, then no new states are added. In fact, intermediate cases are possible, for example, where antibonding states are split around the Fermi level, and in these intermediate cases H can be a partial electron donor or acceptor.

Although it is difficult to discern the exact nature of the bonding, the evidence suggests that H behaves as an electron promoter, adding a small amount of charge to the metal Fermi surface. In the NaCl hydrides a small increase in the charge on the metal ions is seen upon hydriding, and this increase is found primarily in the d orbitals. In fact, the charge increases in exactly those d orbitals with the greatest density at the Fermi surface, strongly suggesting the H has increased occupation of states at the Fermi surface. The impact of these promoted electrons on the formation energy will be discussed further in Sec. V. Furthermore, projected DOS generally show at least some H s and metal e_g character well above the Fermi level and the original metal e_g states. The high-energy H s and metal e_g states are antibonding orbitals of the H and metal and their presence demonstrates that at least some of the antibonding states are above the Fermi level. This is consistent with the fact that for H to promote electrons to the Fermi surface some antibonding states must be above the Fermi level.

Although hydriding causes electron promotion to the Fermi surface of the metal, the H itself also seems to gain some electrons, becoming at least somewhat anionic. In a number of different NaCl structure metal hydrides (TiH, MnH, CoH) we find that H has about 1.1 s electrons in a 1-Å sphere around the atom. This is clearly more than would be expected in the isolated H atom, suggesting anionic character.

The extra electrons needed to increase charge upon hydriding on both the H and the metal come from the interstitial charge density. The rearrangement of the interstitial charge is not surprising given that the hybridization between metals and H seem primarily to involve the free electron band of the metal.

V. HYDRIDE FORMATION ENERGY: RELATION TO THE ELECTRONIC STRUCTURE

Having analyzed the electronic structure we are now in a position to explain the trends in the hydride formation energy in Figs. 1 and 2. The total hydride formation reaction will be broken down in three hypothetical, consecutive reactions, the energy of each of which can be directly related to the electronic structure. The sum of these three reaction energies will be the hydride formation energy. Since most of the structures show the same trend across the transition metal series in Figs. 1 and 2, we focused on the fluorite (CaF_2) and rocksalt (NaCl) structures. Both of these structures can be described in terms of an fcc metal lattice with hydrogen atoms occupying either all of the octahedral sites (NaCl) or all of the tetrahedral sites (CaF_2). The three reactions are the following.

(i) Conversion of the metal from its equilibrium structure (e.g., bcc, fcc, hcp) to fcc, the arrangement of the metal ions in the fluorite and rocksalt structure. This is referred to as the structural effect as it is determined by the topology of the metal ions in the hydride structure.

(ii) Expansion of the metal fcc structure to the lattice parameter of the hydride. This is referred to as the elastic effect.

(iii) Introducing the hydrogen atoms into the interstices of the fcc lattice so as to form the hydride. This is the chemical

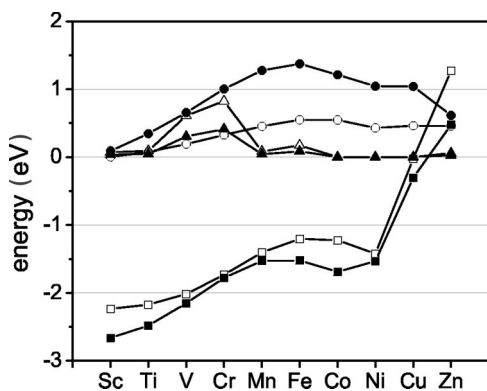


FIG. 8. Energy of the metal in the fcc structure relative to the stable structure (triangles). Energy for expanding the metal from its (meta)stable fcc lattice parameter to the lattice parameter of the hydride (circles). Energy of metal hydride relative to the metal in the expanded fcc structure (squares). Solid symbols correspond to the CaF_2 structure, while open symbols correspond to the NaCl structure (all energies given per H_2 molecule).

effect and is a measure of the bonding between the hydrogen and the metal.

(After submission of this paper, the work of Miwa and Fukumoto²¹ was published, in which a similar but independently derived decomposition of the hydride formation energy was performed. Similar conclusions were drawn²¹ as will be presented below, though here the complete transition-metal series is considered.)

Figure 8 shows the energy of the first reaction for all the metals, the transformation of the metal structure to an fcc structure. For metals such as Co, Ni, and Cu this structural transformation energy is zero, as fcc is their lowest-energy arrangement. Only for V and Cr, two metals with stable bcc structures, is this structural transformation energy significant. The hcp metals, such as Sc and Ti, have only a very small structural transformation energy. All energy values are per 2H in the hydride. For the rocksalt structure one needs twice as many metal atoms to get the same amount of hydrogen as in the fluorite compound, so that the energy in step (i) for rocksalt hydrides is twice as high as for fluorite hydrides. The energetics of steps (ii) and (iii) (shown in Fig. 8) will also be given per 2H. This convention makes it possible to compare all reaction energy on a per H_2 basis.

A large positive contribution to the hydride formation energy comes from step (ii): the expansion of the metal lattice to the lattice parameter of the hydride. This elastic energy contribution, shown in Fig. 8, increases as one moves through the $3d$ series up to about Fe and then decreases slightly. An increase in the energy cost for stretching the metal leads to a reduction in the stability of the hydride. For the fluorite structure the variation in this contribution to the hydride formation energy is nearly one and a half electron volts, indicating that it contributes a substantial part to the variation in hydride energies observed in Figs. 1 and 2.

The energy of the third step, the insertion of the hydrogen into the stretched metal structure, is shown in Fig. 8. This energy contribution is strongly negative and is the energetic reason for hydride formation. The energy gain resulting from

hydride insertion decreases when moving through the transition-metal series, in agreement with much of the trend observed in Figs. 1 and 2. With our calibration for the H_2 energy (which might be somewhat inaccurate) only in Zn is the chemical interaction energy with hydrogen not favorable. In Cu it is marginal. It cannot be excluded that in structural arrangements not considered here, the interaction is more favorable.

Of the three contributions to the hydriding energy the structural effect is the smallest. Given how much emphasis has been put in the past on the chemical-electronic interaction of hydrogen with the transition metal, it is surprising that a large effect for the trend in the formation energy actually arises from the expansion of the metal lattice to adopt the hydride lattice parameter. In particular, for the dihydrides this contribution is essential to understanding the variation of the formation energy among the various metals.

The different components of the hydride formation energy can be understood in terms of the band structure and charge transfer. Since the structural effect is small, we will focus here on the elastic and chemical contributions to the formation energy of the hydrides. The elastic energy penalty for hydride insertion is largely determined by the cohesive energy of the metal. For transition metals the cohesive energy is dominated by the d electrons. For early transition metals, the Fermi level lies in strongly bonding levels near the bottom of the d band. However, there are few d electrons in these early transition metals so that the cohesive energy is rather low. This translates in a high formation energy for the hydride, as there is only a small elastic penalty to pay for hydrogen insertion. Going to the right in the $3d$ series, more bonding levels are filled, increasing the cohesive energy and thereby reducing the magnitude of the hydride formation energy. The late transition metals have the Fermi level in the antibonding states near the top of the d band and the cohesive energy decreases with increasing electron count. For the late transition metals such as Cu, the s states also have to be considered to understand the cohesive energy. Hence, Fig. 8 shows that the elastic contribution to the formation energy of hydrides is important and can be fully rationalized in terms of the cohesive energy of the host metal.

The chemical interaction energy (Fig. 8) varies significantly across the transition metals and is very different for Cu and Zn. For the transition metals the chemical energy component is strongly favorable for hydride formation and decreases from the early to the late transition metals. It is clearly responsible for the lack of stability of Cu and Zn hydrides. As discussed previously, the insertion of hydrogen actually causes electron promotion to the Fermi surface. Therefore, the variation of the chemical energy component across the metal series is likely determined by the location of the Fermi surface. We believe there are two competing factors which contribute to the change in promotion energy as a function of atomic number. Because the d orbitals fill with increasing atomic number, the electron must be promoted to a higher-energy orbital. However, this effect is counterbalanced by an overall lowering of the d orbital energies associated with the increasing nuclear charge. These terms are relatively closely balanced, with the destabilizing effect of

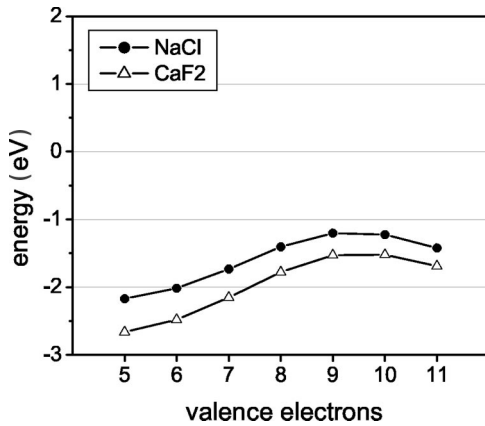


FIG. 9. Chemical contribution to the hydride formation energy as function of the number of valence electrons (energy given per H_2 molecule).

d-band filling winning out from Sc to Fe and the effect of the increasing nuclear charge slightly dominating from Fe to Ni. The dramatic increase in hydride formation energy after Ni is due to the radical rearrangement of the band structure associated with the filled *d* bands of Cu and Zn. The highest electron is forced into a much high-energy orbital. This is very clear in Zn, where the hydride has 13 valence electrons and only 12 states available from the metal *d* and metal-H bonding orbitals. During hydriding, electron promotion occurs to a very-high-energy band, destabilizing the Zn hydride.

The trends in the three components of hydride formation can now be put together to explain the formation energies in Figs. 1 and 2. The early transition metals suffer little loss of cohesive energy from the metal-metal bonds as hydrogen is inserted, but benefit from a large direct H-*M* interaction (Fig. 8). This gives a large negative hydriding energy for these metals. Moving to systems with more *d* electrons, the energy cost of deforming the metal lattice increases and the chemical interaction between hydrogen and metal decreases, so that the stability of the hydride decreases. The apparent local minimum in hydride energy at Mn is due to the strong increase in energy of hydride formation for V and Cr, which are stable bcc metals. For these systems, forming either rock-salt or fluorite hydrides comes with the large cost of rearranging the metal lattice into the less favorable fcc structure (the “structure effect” discussed above). However, it should not be excluded that there is some more stable hydride based on the bcc structure that would lower the formation energy of these hydrides. Actually, while VH_2 has the fluorite structure, with lower hydrogen content, V is known to retain the bcc structure.

For the hydrides of the later transition metals, Co and Ni, the formation energy decreases and the hydrides become somewhat more stable. This is due to a reduction in the contributions from the structural and elastic energies and a fairly flat chemical contribution. However, the metal cohesive energy (and therefore the structural energy) remains quite large, making for an overall weak driving force for hydride formation. For Cu and Zn the hydriding energy again rises sharply, driven by the sharp increase in the chemical energy. For Zn,

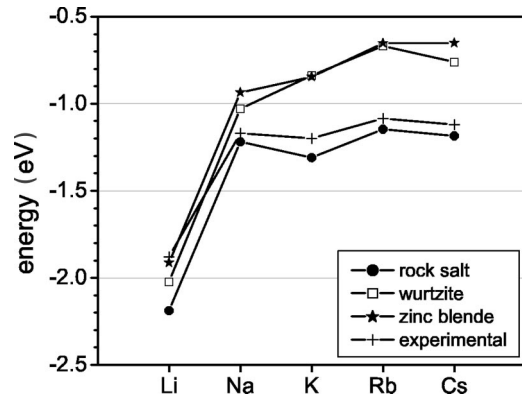


FIG. 10. Formation energy of the group-I metal hydrides in various crystal structures (energy given per H_2 molecule, experimental values taken from Refs. 7 and 23).

our results indicate that even without an elastic and structural energy cost, no stable hydride would form due to the highly positive contribution from the chemical term. Our observation that the cohesive energy of the metal plays a key role in the formation energy of the hydride gives a more fundamental justification for Miedema’s “law of inverse stability.”¹⁸ Miedema observed that the more stable the alloy, the less stable the hydride. He attempted to explain this on the basis of his deformable atom model.²² Our analysis indicates that this rule is simply a restatement of what can be observed when comparing Figs. 8 and 1. When the metal is very stable (has high cohesive energy) the stretching of the metal-metal bonds, necessary for hydride formation, comes at a high energy cost. The stronger this effect, the lower the hydride formation energy.

Figure 9 offers a further illustration of the importance of the valence electron count for the chemical hydrogen insertion energy. It shows the chemical component of the hydrogen insertion energy as function of the number of valence electrons ($s + d$) for the hydrides in both the fluorite (MH_2) and rocksalt (MH) structures. Effectively, this corresponds to shifting the fluorite hydrides in Fig. 8 to the right by one position as it has one valence electron more than the hydrides with the rocksalt structures. With this shift, the chemical binding trends are parallel, confirming that this contribution to the formation energy is largely determined by the position of the Fermi level.

VI. GROUPS I AND II

A. Group I

Figure 10 shows the hydride formation energy in the rock-salt, wurtzite, and zinc-blende structures for the alkali metals. The variation of formation energy with metal is similar for all the structures. The most notable feature is the large energy difference between lithium hydride and the other group-I hydrides. We believe this to be due to hybridization between the Li *s* and the hydrogen *s*. Figures 11(a) and 11(b) show the density of states for LiH and KH. KH was chosen as typical for the other group-I hydrides. For lithium there is a wide band below the Fermi level. For KH this band is

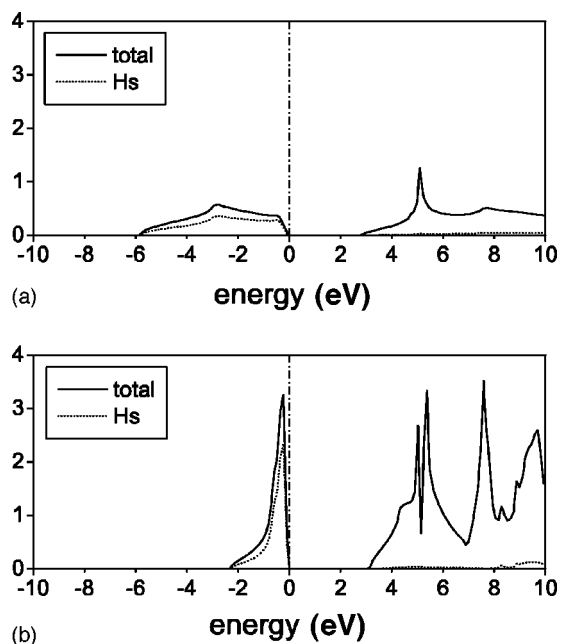


FIG. 11. Density of states for LiH (a) and KH (b) in the rocksalt structure.

much narrower and has a large peak just below the Fermi level. We confirmed that the densities of states of the other group-I hydrides are similar to that of KH (i.e., that they have a narrow band below the Fermi energy). The broadband in LiH arises from the similarity of the Li $2s$ and hydrogen $1s$ orbital in energy and size, allowing for a significant hybridization. In the heavier group-I hydrides the metal s energy is mismatched with the hydrogen $1s$, leading to a smaller bandwidth and lower stability compared to LiH.

B. Group II

Figure 12 shows the hydride formation for the group-II metals. The group-II metal hydrides behave quite differently from the group-I hydrides. From beryllium to calcium the hydride formation energy becomes more negative and from Ca to Ba it is relatively constant. The high energy of beryllium hydride can be explained by the fact that it is a very stable metal (the cohesive energy is about 2 eV more stable than the rest of the group-II metals). This means that the hydride is considerably less stable than the others. The trend from Mg to Ba with the minimum at Ca is more difficult to explain. Given that these hydrides are very ionic, the minimum at Ca could represent the optimal balance between cohesive energy of the metal (which favors hydrides of the heavy earth alkali metals), and the electrostatic energy between the H^- and M^+ ions (which is lowest in the light earth alkalis as they have a smaller lattice parameter).

C. Comparison to experimental formation Energies

The experimental formation enthalpies for group-I and -II hydrides are shown in Figs. 10 and 12. The data are mostly taken from Ref. 23, except for BeH, which is taken from Ref. 7. We only show comparisons for the group-I and -II hy-

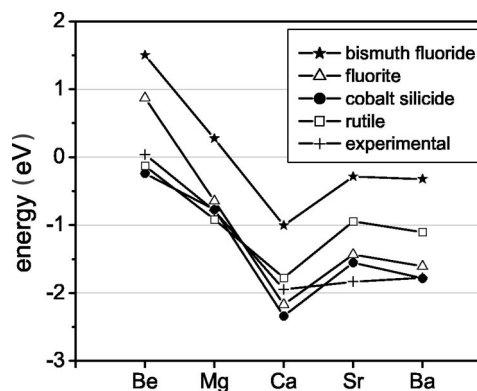


FIG. 12. Formation energy of the group-II metal hydrides in various crystal structures (energy given per H_2 molecule, experimental values taken from Refs. 7 and 23).

drides as there are very little reliable experimental data for the transition-metal hydrides in the appropriate composition range. Both in absolute value and in qualitative trend, there is good agreement between the calculated and measured formation enthalpies. Even the dip for K between Na and Rb is well represented in the calculated values for the alkali hydrides. The absolute values are somewhat different but this is likely due to our inaccurate reference for the energy of the H_2 gas as explained previously. All alkali hydrides are stable in the rocksalt structure in agreement with our prediction.

Similarly, the agreement between experimental information and calculated energies is good for the group-II hydrides. CaH_2 , SrH_2 , and BaH_2 are correctly predicted to form in the Co_2Si structure, while MgH_2 is the only one of the earth alkalis that forms the rutile structure. The structure of Be hydride is complex and not fully characterized so that comparison with the calculations on a limited number of structures is not meaningful.

VII. CONCLUSIONS

We have systematically investigated the electronic structure and formation energy of hydrides and analyzed the relationship between the two. For the alkali and alkali-earth metals hydrogen insertion introduces a hydrogen s state below the Fermi level. In lithium hydride this band is quite wide, explaining lithium hydride's unusual stability. Similarly, in the transition metals, an s band of predominant hydrogen character appears below the Fermi level upon hydrogen insertion. Hydrogen is shown to be somewhat anionic, in addition to the fact that hydrogen insertion actually causes electron promotion to the Fermi surface. By breaking down the hydride formation energy into three steps, it is possible to rationalize trends across the transition-metal series. The two largest contributions to the hydride formation energy are the chemical effect (negative) due to the hydrogen insertion and the elastic effect (positive) due to the expansion of the metal framework. The chemical effect provides all the stabilization for the hydride and generally grows more positive (less stabilizing) across the transition-metal series. A dramatic increase in the chemical contribution is responsible for the lack of stability of hydrides of Cu and Zn. However, the elastic

effect is approximately the same size as the chemical effect and also has an important influence on the hydride formation energy trends through the transition metals.

How can these observations be used to design hydrides with appropriate stability? The chemical effect can be influenced somewhat by tailoring the position and density of states at the Fermi level. A more effective way of influencing the formation energy of hydrides may be through the cohesive energy of the host metal. As we demonstrated, this is a large factor in the stability of the hydride. For designing hydrides with marginal stability (so that hydrogen can be released easily) this may be the most promising direction, as the cohesive energy of alloys can be varied over wide ranges through compositional modification. In addition, this is a quantity that can be rapidly predicted for a large number of alloys with the first principles methods used in this work.

Obviously, it should be realized that the formation energy is only one important parameter for a hydride to be useful as

a hydrogen source or for reversible hydrogen storage. Hydrogen diffusion, maximal hydrogen content, oxidation resistance, cost, and weight are other important factors.

ACKNOWLEDGMENTS

This work was funded through the Laboratory for Energy and the Environment at the Massachusetts Institute of Technology and by the Department of Energy under Contract No. DE-FG0296ER45571. Computing resources were provided by the National Partnership for Advanced Computing Infrastructure (NPACI). H.S. acknowledges support from the Cambridge-MIT Institute for supporting his stay at MIT. This research was supported in part by NSF cooperative agreement No. ACI-9619020 through computing resources provided by the National partnership for Advanced Computational Infrastructure at the San Diego Supercomputer Center.

-
- ¹H. Vehoff, in *Hydrogen in Metals III, Properties and Applications*, edited by H. Wipf (Springer-Verlag, Berlin, 1997), Vol. 73, p. 215.
- ²Z.A. Schlapbach, *Nature (London)* **414**, 353 (2001).
- ³O.A. Guthrie, *J. Alloys Compd.* **295**, 889 (1999).
- ⁴J.P. Bastide, B. Bonnetot, J.M. Letoffe, and P. Claudy, *Mater. Res. Bull.* **15**, 1215 (1980).
- ⁵J.A. Goedkoop and A.F. Andresen, *Acta Crystallogr.* **7**, 672 (1954).
- ⁶E. Wiberg, W. Henle, and R. Bauer, *Chem. Ber.* **85**, 593 (1951).
- ⁷G. G. Libowitz, *The Solid-State Chemistry of Binary Metal Hydrides* (Benjamin, New York, 1965).
- ⁸C.G. Shull, E.O. Wollan, G.A. Morton, and W.L. Davidson, *Phys. Rev. B* **73**, 842 (1948).
- ⁹A.C. Switendick, *J. Less-Common Met.* **130**, 249 (1987).
- ¹⁰A.C. Switendick, *Solid State Commun.* **1463**, 8 (1970).
- ¹¹M. Gupta, *J. Less-Common Met.* **103**, 325 (1984).
- ¹²W. E. Wallace and S. K. Malik, in *Hydrides for Energy Storage* edited by A. F. Andresen and A. J. Maelands (Pergamon, New York, 1978), pp. 33–40.
- ¹³D.A. Papconstantopoulos and A.C. Switendick, *J. Less-Common Met.* **103**, 317 (1984).
- ¹⁴I. Baraille, P.C.M. Causa, and C. Pisani, *Chem. Phys.* **179**, 39 (1994).
- ¹⁵R. Yu and P.K. Lam, *Phys. Rev. B* **37**, 8730 (1988).
- ¹⁶W. Wolf and P. Herzig, *J. Phys.: Condens. Matter* **12**, 4535 (2000).
- ¹⁷M. Gupta, *J. Alloys Compd.* **293-295**, 190 (1999).
- ¹⁸A.R. Miedema, *J. Less-Common Met.* **32**, 117 (1973).
- ¹⁹G. Kresse and J. Furthmuller, *Comput. Mater. Sci.* **6**, 15 (1996).
- ²⁰G. Kresse and J. Hafner, *Phys. Rev. B* **47**, 558 (1993).
- ²¹K. Miwa and A. Fukumoto, *Phys. Rev. B* **65**, 155114 (2002).
- ²²F. R. de Boer, R. Boom, W. C. M. Matten, A. R. Miedema, and A. K. Niessen, in *Cohesion in Metals: Transition Metal Alloys*, edited by F. R. de Boer and D. G. Pettifor, (North-Holland, Amsterdam, 1988), Vol. 1.
- ²³*Metal Hydrides*, edited by W. M. Mueller, J. P. Blackledge, and G. G. Libowitz, (Academic Press, New York, 1968).
- ²⁴G. Libowitz, *J. Nucl. Mater.* **2**, 1-22 (1960).